Landau-Lifshitz-Bloch Approach for Magnetization Dynamics Close to Phase Transition

41

Oksana Chubykalo-Fesenko and Pablo Nieves

Contents

Abstract

Micromagnetic modeling has recommended itself as a useful tool for the design of magnetic nanostructures in multiple applications. The standard micromagnetics based on the integration of the Landau-Lifshitz-Gilbert equation is a valid approach at low temperatures only. In multiple recent applications such as heat-assisted magnetic recording or ultrafast magnetic dynamics, the temperatures often go close to the Curie temperature T_c and above. Here we review the micromagnetic approach valid in this temperature range, based on the use

O. Chubykalo-Fesenko (✉)
Instituto de Ciencia de Materiales de Madrid, Spanish National Research Council – CSIC, Madrid, Spain
e-mail: oksana@icmm.csic.es

P. Nieves
International Research Center in Critical Raw Materials and Advanced Industrial Technologies, Universidad de Burgos, Burgos, Spain

W. Andreoni, S. Yip (eds.), *Handbook of Materials Modeling*,
https://doi.org/10.1007/978-3-319-44677-6_72

of the Landau-Lifshitz-Bloch equation. The essential part of this approach is the presence of the temperature-dependent longitudinal relaxation with the characteristic time diverging at T_c. We review this approach in its classical and quantum formulations and for one- and two-component materials. The behavior of longitudinal relaxation time is discussed. Finally, we present examples of the use of this micromagnetics related to the modeling of ultrafast magnetization dynamics.

1 Introduction

Recent advances in magnetism including the design of novel nanostructured magnetic materials, better theoretical understanding of magnetic phenomena, and the development of nanoscale experimental techniques have driven the progress of nanotechnology in general but specially in the data storage industry. Recently, novel high-temperature magnetic phenomena have been discovered and attracted a lot of researchers. One of them is the laser-induced ultrafast magnetization dynamics (see, e.g., Beaurepaire et al. 1996; Vahaplar et al. 2009; Kirilyuk et al. 2010) where a subpicosecond dynamics is observed when a femtosecond laser pulse is applied to magnetic materials. Another example is the spin Seebeck effect (Uchida et al. 2008) where spin currents and spin accumulation are observed in a ferromagnet due to a temperature gradient. Apart from their fundamental interest, these phenomena are very appealing from technological perspectives that range from increasing the speed of the magnetization switching to the production of spin-voltage generators. It has been also found that a good strategy to improve the performance of hard disk devices and magnetic random-access memories is to increase the temperature of the magnetic thin film during the writing process. Therefore, it is necessary to search for models that can describe the magnetic behavior in these novel high-temperature phenomena, in which temperature is often raised up to and above the Curie temperature T_c.

In magnetism, micromagnetic modeling is a very useful complement to experimental measurements, especially for calculations of hysteresis and dynamics of magnetic nanostructures such as magnetic thin films, dots, stripes, etc. (Brown 1963a; Fidler and Schrefl 2000; Chantrell et al. 2001). The micromagnetics is essentially a macroscopic continuous theory. It uses a discretization of continuous magnetization function in finite elements or finite differences. The dynamics of each unit in standard micromagnetics is based on the integration of the classical Landau-Lifshitz-Gilbert (LLG) equation of motion (Landau and Lifshitz 1935; Gilbert 2004). It is essentially a zero-temperature equation, although the micromagnetic parameters could be taken as experimentally measured values at a given temperature T. The temperature effects are typically included by adding random fields acting on each discretization element with properties consistent with the thermodynamical equilibrium (Brown 1963b; Chubykalo et al. 2003). However, this approach is correct only for low temperatures and largely overestimates the transition temperature T_c (Grinstein and Koch 2003), since the magnitude

of the magnetization vector in each element is constant. At high temperatures, high-frequency spin waves, responsible for longitudinal magnetization fluctuations near the Curie temperature T_c, are cut, and the value of the Curie temperature is strongly overestimated. To solve this issue, an alternative micromagnetic approach for higher temperatures based on the Landau-Lifshitz-Bloch (LLB) equation has been proposed (Garanin 1997; Chubykalo-Fesenko et al. 2006) where the magnitude of the magnetization vector is not conserved at each discretization element and the longitudinal magnetization fluctuations are introduced.

Furthermore, a complete description of the material's magnetic behavior requires very different spatial scales going from Ångström (like microscopic interactions at atomic level) to macroscale (magnetic domains typically have micrometer sizes) and also very different timescales going from femtoseconds (as in the ultrafast magnetization dynamics) to years (thermal stability in magnetic storage media). The ab initio models typically calculate microscopic parameters of the material, while atomistic spin (Heisenberg) models are good to describe the phase transitions. However, to model realistic devices such as sensors or magnetic recording head performance, large-scale modeling based on the micromagnetics is used. One way to include the effects of the microscopic properties on the magnetic macroscopic behavior is the multiscale approach (Kazantseva et al. 2008a; Atxitia et al. 2010b; Hinzke et al. 2015). Namely, ab initio calculations (the most widely used formalism is density functional theory (DFT)) are used to calculate the intrinsic parameters as magnetic moment (μ), exchange constants (J), on-site magnetocrystalline anisotropy (k), etc…; then these parameters are used in atomistic classical (Heisenberg-like) models where the temperature dependence of the equilibrium magnetization $M_s(T)$, anisotropy $K(T)$, and exchange stiffness $A(T)$ among other properties can be calculated; and finally the temperature dependence of these parameters is included in the micromagnetic approach which can model the magnetic behavior at large spatial scale (see the sketch in Fig. 1). The temperature is an essential part of this approach, and the correct micromagnetic description is based on the LLB equation (Kazantseva et al. 2008a).

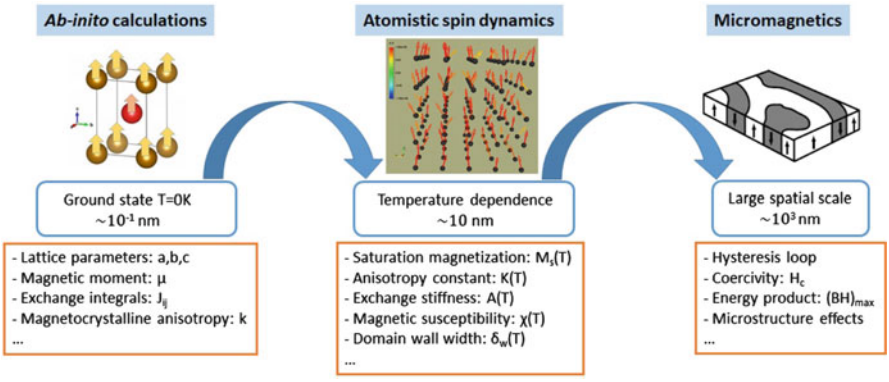

Fig. 1 The sketch of the multiscale approach

The micromagnetic modeling based on the LLB equation has manifested itself as a good approach to model new phenomena such as the ultrafast magnetization dynamics (Kazantseva et al. 2008a; Sultan et al. 2012; Atxitia et al. 2007, 2010a, 2016; Mendil et al. 2014), spin caloritronics (Hinzke and Nowak 2011; Schlickeiser et al. 2014), and heat-assisted magnetic recording (McDaniel 2012; Greaves et al. 2015; Takano et al. 2011; Vogler et al. 2014, 2016) processes.

2 Classical Micromagnetic Models

2.1 The Classical Heisenberg (Atomistic) Modeling

The magnetic moments in the solid state can be localized or semi-localized, carried by the conduction electrons (itinerant magnetism) like in metals. However, models based on a classical Heisenberg Hamiltonian of localized spins are currently used to describe the magnetic properties in both situations. Typically, the generalized Heisenberg Hamiltonian for a uniaxial magnet in these atomistic models is written as

$$\mathcal{H} = -\sum_i \mathbf{H}\cdot\boldsymbol{\mu}_i - \sum_i k_i s_{i,z}^2 - \frac{1}{2}\sum_{i,j} J_{ij}\mathbf{s}_i\cdot\mathbf{s}_j, \tag{1}$$

where $\mathbf{H}$ is the external magnetic field, $\boldsymbol{\mu}_i$ is the magnetic moment per atom at site i, $\mathbf{s}_i = \boldsymbol{\mu}_i/\mu_i$, k_i is the uniaxial atomic-site anisotropy constant, and J_{ij} is the exchange constant between the spins i and j. The first term in Eq. (1) corresponds to the Zeeman energy, the second term is the on-site uniaxial magnetocrystalline anisotropy energy (where the uniaxial axis is along the z-axis), and the last one is the exchange energy. The exchange energy may be long-range corresponding to the RKKY interactions and site-dependent. The dynamics of each normalized classical atomic magnetic moment $\mathbf{s}_i$ is described using the phenomenological Landau-Lifshitz-Gilbert (LLG) equation given by

$$\frac{d\mathbf{s}_i}{dt} = -\frac{\gamma}{1+\lambda^2}(\mathbf{s}_i\times\mathbf{H}_{\mathrm{eff},i}) - \frac{\gamma\lambda}{(1+\lambda^2)}\mathbf{s}_i\times(\mathbf{s}_i\times\mathbf{H}_{\mathrm{eff},i}), \tag{2}$$

where γ is the gyromagnetic ratio, λ is called atomic coupling to the bath (atomistic damping) parameter, $\mathbf{H}_{\mathrm{eff},i} = -\partial\mathcal{H}/\partial\boldsymbol{\mu}_i$ is the effective field, and $\mathcal{H}$ is the Hamiltonian given by Eq. (1). Equation (2) is a deterministic equation; it means that given the same initial conditions, one obtains always exactly the same dynamics. However, the atomic magnetic moment in a solid follows a stochastic dynamics due to the interaction with its surroundings. This fact is included in Eq. (2) adding a stochastic field $\boldsymbol{\zeta}_i$ to the effective field $\mathbf{H}_{\mathrm{eff},i}$, that is,

$$\frac{d\mathbf{s}_i}{dt} = -\frac{\gamma}{1+\lambda^2}(\mathbf{s}_i\times(\mathbf{H}_{\mathrm{eff},i}+\boldsymbol{\zeta}_i)) - \frac{\gamma\lambda}{(1+\lambda^2)}\mathbf{s}_i\times(\mathbf{s}_i\times(\mathbf{H}_{\mathrm{eff},i}+\boldsymbol{\zeta}_i)), \tag{3}$$

where the stochastic field has the following time average properties following the Brown's theory for nanoparticles (Brown 1963b)

$$\langle \zeta_{i,k} \rangle = 0, \quad \langle \zeta_{i,k}(0)\zeta_{i,k'}(t) \rangle = 2\frac{\lambda k_B T}{\gamma \mu_i}\delta_{kk'}\delta(t), \quad k, k' = x, y, z, \tag{4}$$

where k_B is the Boltzmann constant and δ is Kronecker delta symbol. This approach is called atomistic spin dynamics (ASD) (Skubic et al. 2008; Evans et al. 2014; Eriksson et al. 2017). The macroscopic magnetization at time t is obtained as an average of the atomic magnetic moments over some volume V

$$\mathbf{M}(t) = \frac{1}{V}\sum_{i=1}^{N} \boldsymbol{\mu}_i(t), \tag{5}$$

where N is the total number of atomic magnetic moments inside the volume V.

Simulations based on ASD is a powerful tool to describe the magnetic behavior of magnetic materials. Importantly, the ASD simulations lead to a good agreement with the experimentally measured Curie temperatures. Unfortunately, the size of a magnetic material that can be simulated using ASD is very limited (typically up to $(20–30\,\text{nm})^3$ due to a large number of differential equations that must be numerically integrated.

2.2 Classical Micromagnetic Models at Low Temperatures

A suitable approach to study the behavior of magnetic materials at large scale is micromagnetics. It is based on the continuum approximation where the length scales considered are large enough for the atomic structure of the material to be ignored and small enough to resolve magnetic structures such as domain walls or vortices. In the continuum approximation the macroscopic magnetization is assumed to be a spatial continuous function over the material

$$\mathbf{M}(\mathbf{r}) = M_s \mathbf{m}(\mathbf{r}), \tag{6}$$

where $|\mathbf{m}(\mathbf{r})| = 1$ and M_s is the saturation magnetization. In this approach the energy of a uniaxial magnetic system reads (e.g., Coey 2009)

$$E = \int_V d\mathbf{r}\{-\mathbf{M}\cdot\mathbf{H} - Km_z^2 + A(\nabla\mathbf{m})^2 - \frac{1}{2}\mathbf{M}\cdot\mathbf{H}_d\}, \tag{7}$$

where K is the macroscopic uniaxial anisotropy constant, A is the exchange stiffness parameter, $(\nabla\mathbf{m})^2 = (\nabla m_x)^2 + (\nabla m_y)^2 + (\nabla m_z)^2$, ∇ is the gradient operator, and $\mathbf{H}_d$ is the magnetostatic field which must be calculated self-consistently.

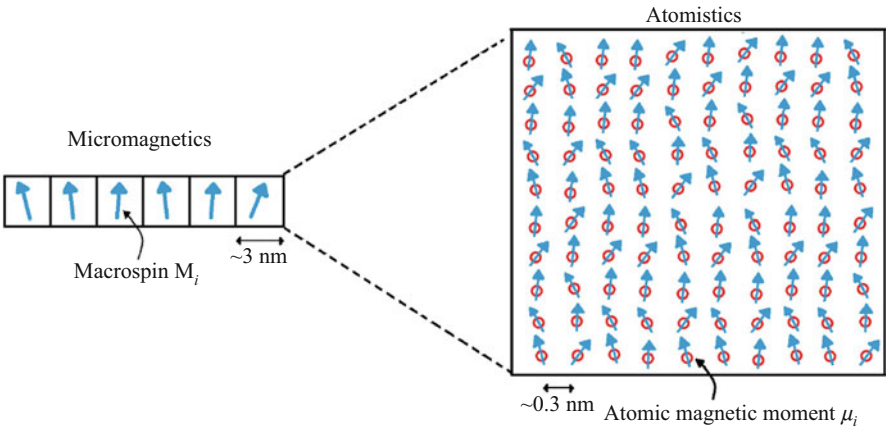

Fig. 2 Illustration of the relation between atomistic model and micromagnetics. (Reprinted from Nieves 2015)

In order to solve micromagnetic problems numerically, the system is divided in cells of volume V_i (typically around few nm^3), and then the average magnetization of the cell at position $\mathbf{r}_i$ is represented by vector called macrospin (see Fig. 2), $\mathbf{M}(\mathbf{r}_i) = \mathbf{M}_i = M_s \mathbf{m}_i$. In a coarse-grained (multiscale) approach, the mascrospin is the average of atomic spin moments in the sense of Eq. (5). In order to choose a suitable volume cell, it is important to take into account the domain wall width parameter δ and the exchange length l_{ex} which are given by

$$\delta = \pi \sqrt{\frac{A}{K}} \ , \qquad l_{\text{ex}} = \sqrt{\frac{A}{M_s^2}}. \tag{8}$$

The domain wall width parameter corresponds to the width of a Bloch wall that is found in magnetic materials with a large magnetocrystalline anisotropy. The exchange length is the length below which atomic exchange interactions dominate typical magnetostatic fields, and it is proportional to the Néel domain wall width. The discretization length must be less than the domain wall width but includes enough atoms to be valid as the continuous approximation. The main difficulty of micromagnetics is the correct calculation of the long-range magnetostatic fields.

The standard dynamic micromagnetics is based on the same LLG equation as in the atomistic approach (however with more justified damping form) for the macrospin $\mathbf{M}_i$ given by

$$\frac{d\mathbf{M}_i}{dt} = -\frac{\gamma}{1+\alpha_{\text{LLG}}^2}(\mathbf{M}_i \times \mathbf{H}_{\text{eff},i}) - \frac{\gamma \alpha_{\text{LLG}}}{(1+\alpha_{\text{LLG}}^2) M_s} \mathbf{M}_i \times (\mathbf{M}_i \times \mathbf{H}_{\text{eff},i}), \tag{9}$$

where α_{LLG} is called the LLG damping (not to be confused with the microscopic damping in the atomistic approach, often designated with the same letter α but called

here λ in order to stress the difference) and $\mathbf{H}_{\text{eff},i}$ is the effective field which is given by

$$\mathbf{H}_{\text{eff},i} = -\frac{1}{V_i}\frac{\partial E}{\partial \mathbf{M}_i} = \mathbf{H}_i + \frac{2K_i m_{i,z}}{M_s}\mathbf{e}_z + \frac{2A_i}{M_s}\nabla^2 \mathbf{m}_i + \mathbf{H}_{d,i}. \tag{10}$$

The temperature effects in micromagnetism are typically included in the following way:

(i) *Via temperature-dependent parameters:* The parameters $M_s(T)$, $A(T)$, $K(T)$, $\alpha_{\text{LLG}}(T)$ are taken at given temperature. Importantly the damping parameter α_{LLG} is also temperature-dependent which is frequently forgotten. As it was mentioned in the introduction, their temperature dependence can be calculated numerically using ASD within the multiscale approach; a detailed explanation of this calculation can be found, for example, in Kazantseva (2008) for FePt. They can also be obtained theoretically, for example, using the mean-field approximation (MFA) or measured experimentally.

(ii) *Via thermal field:* In 1963 W.F. Brown (1963b), considering the superparamagnetism problem in a collection of non-interacting nanoparticles, suggested to include thermal fluctuations in the LLG dynamical equation as stochastic fields whose properties are defined by the equilibrium solution of the corresponding Fokker-Planck (FP) equation. Importantly, these fields are just formal quantities and do not have physical sense; they are used in order to produce stochastic deviations of different magnetization trajectories from their averaged value with correct statistical properties. In 1993 Lyberatos and Chantrell (1993) for the first time studied the dynamics of two interacting magnetic dipoles including these fluctuating thermal fields. This idea was further developed by many authors (Nakatani et al. 1997; García-Palacios and Lázaro 1998; Scholz et al. 2001; Chubykalo et al. 2002). It was shown that the stochastic fields remain uncorrelated and with the same properties for the interacting case (Chubykalo et al. 2003). These developments lead to Langevin dynamics micromagnetics where a fluctuating thermal field $\boldsymbol{\zeta}_i$ is added to the effective field given by Eq. (10) with the following time average properties (the same as used in the ASD dynamics)

$$\langle \zeta_{i,k} \rangle_t = 0, \quad \langle \zeta_{i,k}(0)\zeta_{i,k'}(t) \rangle_t = 2\frac{\alpha_{\text{LLG}} k_B T}{\gamma M_s V_i}\delta_{kk'}\delta(t), \quad k, k' = x, y, z. \tag{11}$$

The main feature of this approach is that the magnitude of every macrospin is conserved in all dynamical processes, that is, $|\mathbf{M}_i|$ =const. However, the direct comparison with the ASD shows that thermal simulations of the magnetization dynamics based on the micromagnetic LLG equation are not suitable for high temperatures (Chubykalo-Fesenko et al. 2006). This is due to the fact that micromagnetic simulations do not include the high-frequency spin waves, and, thus, the Curie temperature is seriously overestimated (Grinstein and Koch 2003). Additionally, in recent ASD simulations (Chubykalo-Fesenko et al. 2006; Kazantseva et al. 2007),

it has been demonstrated that at high temperatures several important effects occur which cannot be taken into account in the micromagnetic LLG approach. Namely, during the magnetization dynamics, (i) the magnetization vector magnitude is not conserved, (ii) longitudinal magnetization relaxation occurs with the longitudinal relaxation time increment approaching T_C (known as critical slowing down), and (iii) at the same time the transverse relaxation time decreases (Chubykalo-Fesenko et al. 2006). Therefore, a different micromagnetic approach is required at elevated temperatures.

2.3 Thermal Micromagnetics at High Temperatures

In 1997 an alternative approach was suggested by D. Garanin (1997). Based on the Fokker-Planck equation, he derived a classical macroscopic equation of motion for the magnetization called Landau-Lifshitz-Bloch (LLB) equation. The name was chosen in order to stress that the magnetization behavior interpolates between the Landau-Lifshitz equation at low temperatures (micromagnetic LLG Eq. (9)) and the well-known Bloch equation (Bloch 1946) at high temperatures. The Bloch equation is a phenomenological equation frequently used in the nuclear spin resonance description, for example, for protons in a water molecule. The dynamical equation for the ensemble of paramagnetic spins involves the same precessional term and two phenomenological relaxational parameters describing the longitudinal relaxation (defined by the characteristic time T_1) and the transverse relaxation (T_2). In the nuclear spin resonance case $T_2 \ll T_1$, for ferromagnetic materials of the interest here, the situation is the opposite due to a dominant role of large exchange interactions.

The derivation of the classical LLB assumes the classical atomistic approach (ASD) of Sect. 2.1, only based on the Landau-Lifshitz (LL) equation instead of the LLG (i.e., disregarding the term λ^2 in Eq. (2), which anyway is small). First, the Fokker-Planck equation corresponding to many-spin Eq. (9) was calculated in Garanin (1997) (see also details in Atxitia 2012). Using the dynamics of the probability function, governed by this equation and disregarding the third-order moment distribution, one obtains an equation for thermal average of the spin polarization, i.e., the reduced magnetization $\mathbf{m} =< \mathbf{s}_i >$ in a paramagnetic state. For the treatment of ferromagnet, the external field is substituted by the mean field.

The corresponding LLB equation for $\mathbf{m}$ has the following form (see details in Garanin 1997 and Atxitia 2012):

$$\frac{d\mathbf{m}}{dt} = -\gamma[\mathbf{m} \times \mathbf{H}^{\mathrm{MFA}}] - \Gamma_{\parallel}\left(1 - \frac{\mathbf{m}\mathbf{m}_0}{m^2}\right)\mathbf{m} - \Gamma_{\perp}\frac{[\mathbf{m} \times [\mathbf{m} \times \mathbf{m}_0]]}{m^2}, \tag{12}$$

where

$$\mathbf{m}_0 = L(\xi)\frac{\boldsymbol{\xi}}{\xi}, \quad \boldsymbol{\xi} \equiv \beta\mu\mathbf{H}^{\mathrm{MFA}}, \quad \mathbf{H}^{\mathrm{MFA}} = \frac{zJ}{\mu}\mathbf{m} + \mathbf{H}'. \tag{13}$$

Here $\xi \equiv |\boldsymbol{\xi}|$, $L(\xi) = \coth(\xi) - 1/\xi$ is the Langevin function, $\beta = 1/k_B T$, k_B is the Boltzmann constant; μ is the atomic magnetic moment; z is the number of nearest neighbors; J is the Heisenberg exchange interaction parameter; $\mathbf{H}'$ contains the external magnetic field and the nonhomogeneous part of the exchange interaction;

$$\Gamma_{\parallel} = \Lambda_N \frac{L(\xi)}{\xi L'(\xi)}, \quad \Gamma_{\perp} = \frac{\Lambda_N}{2}\left(\frac{\xi}{L(\xi)} - 1\right) \tag{14}$$

describe parallel and perpendicular relaxation rates, respectively; $\Lambda_N = 2\gamma\lambda k_B T/\mu$ is the characteristic diffusion relaxation rate or, for the thermo-activation escape problem, the Néel attempt frequency; and $L'(\xi) = dL/d\xi$ is the derivative of the Langevin function. This equation can be already used for modeling and in many cases gives even a better agreement with the ASD than a more conventional LLB equation presented below.

To put this equation in the form, similar to the LLG one, the homogeneous part of the exchange field is assumed to be much larger than all other fields acting in the system ($[zJ/\mu]m \gg H'$). This leads to the conventional form of the LLB equation which in micromagnetics is written for each discretization element (macrospin) i

$$\frac{d\mathbf{m}_i}{dt} = -\gamma\left[\mathbf{m}_i \times \mathbf{H}^i_{\text{eff}}\right] + \frac{\gamma\alpha_{\parallel}}{m_i^2}\left(\mathbf{m}_i \cdot \mathbf{H}^i_{\text{eff}}\right)\mathbf{m}_i - \frac{\gamma\alpha_{\perp}}{m_i^2}\left[\mathbf{m}_i \times \left[\mathbf{m}_i \times \mathbf{H}^i_{\text{eff}}\right]\right], \tag{15}$$

where $\mathbf{m}_i = \mathbf{M}_i/M_e(0)$ with $M_e(0) = M_s(0)$ being the equilibrium saturation magnetization at $T = 0K$. The longitudinal and transverse relaxation parameters are

$$\alpha_{\parallel} = \lambda\frac{2T}{3T_c}, \qquad \alpha_{\perp} = \lambda \cdot \begin{cases} \left[1 - \frac{T}{3T_c}\right] & T \lesssim T_c, \\ \frac{2T}{3T_c} & T \gtrsim T_c. \end{cases} \tag{16}$$

Note that in the alternative representation, the magnetization can be normalized at its value at T, i.e., using $\mathbf{n}_i = \mathbf{M}_i/M_e(T)$ as is typically done for the LLG micromagnetics. This leads to the same form of the LLB equation but now for the variable $\mathbf{n}_i$. The only difference is the renormalization of the damping parameters by the factor $m_e = M_e(T)/M_e(0)$. Since $m_e \to 0$ at T_c, this form of the LLB equation is obviously not useful for modeling near the phase transition but should be used for the comparison with the LLG micromagnetic modeling.

In the LLB-based micromagnetic approach, the effective fields are given by

$$\mathbf{H}^i_{\text{eff}} = \mathbf{H} + \mathbf{H}_{i,\text{EX}} + \mathbf{H}_{i,A} + \begin{cases} \frac{1}{2\tilde{\chi}_{\parallel}}\left(1 - \frac{m_i^2}{m_e^2}\right)\mathbf{m}_i & T \lesssim T_c, \\ \frac{J_0}{\mu}\left(1 - \frac{T}{T_c} - \frac{3m_i^2}{5}\right)\mathbf{m}_i & T \gtrsim T_c, \end{cases} \tag{17}$$

where $\widetilde{\chi}_{\parallel} = (\partial m/\partial H)_{H\to\infty}$ is the reduced longitudinal susceptibility and J_0 is the zero Fourier component of the exchange interaction which is related to the Curie temperature T_c in the MFA through $T_c = J_0/(3k_B)$ (in the simple cubic lattice case with nearest interactions only $J_0 = 6J$). The last term in Eq. (17) describes the internal exchange field inside the macrospin. $\mathbf{H}$ is the applied magnetic field and $\mathbf{H}_{i,\mathrm{EX}}$ is exchange interaction between macrospins, and it is given by

$$\mathbf{H}_{i,\mathrm{EX}} = \frac{2A_i(T)}{m_i^2 M_s(0)}\nabla^2\mathbf{m}_i = \frac{2A_i(T)}{m_i^2 M_s(0)\triangle^2}\sum_{\langle i,j\rangle}\left(\mathbf{m}_j - \mathbf{m}_i\right), \tag{18}$$

where $\langle i, j\rangle$ means a sum over neighbors, $\triangle$ is the lateral size of the micromagnetic discretization cell, $A_i(T)$ is the micromagnetic exchange also called stiffness parameter, and $\mathbf{H}_{i,A}$ is the anisotropy field given by

$$\mathbf{H}_{i,A} = -\frac{1}{\widetilde{\chi}_{\perp}}\left(m_{i,x}\mathbf{e}_x + m_{i,y}\mathbf{e}_y\right), \tag{19}$$

where $\widetilde{\chi}_{\perp}$ is the reduced transverse susceptibility. Note that the use of the transverse susceptibility is more physically correct as that of the anisotropy (see discussion in Garanin and Chubykalo-Fesenko 2004). However, in practice the anisotropy notion is still used in most of cases, i.e., one assumes $\widetilde{\chi}_{\perp}(T) = M^2/[2K(T)]$.

The LLB equation contains six temperature-dependent parameters: $\lambda(T)$, $M_e(T)$, $A(T)$, $K(T)$, $\widetilde{\chi}_{\parallel}(T)$, and $\widetilde{\chi}_{\perp}(T)$. Typically, the parameter λ is considered in ASD temperature independent. This however is not true in the ab initio modeling (see also discussion in Nieves et al. 2014). In principle other parameters can be measured experimentally. In the multiscale approach the temperature dependence of $M_e(T)$, $A(T)$ and $K(T)$ is calculated using ASD (Kazantseva et al. 2008a; Atxitia et al. 2010b; Nieves et al. 2017), and the scaling with magnetization relations can be used for the last two of them (Kazantseva 2008; Atxitia et al. 2010b; Moreno et al. 2016; Asselin et al. 2010). The parameter $M_e(T)$ can be also obtained using the MFA as the solution of the equation $m_e = L(\beta J_0 m_e)$ where $L(x) = \coth(x) - 1/x$ is the Langevin function. The exchange parameter J_0 can be calculated by first principles or roughly estimated by MFA expression $J_0 = 3k_B T_c$ using experimental Curie temperature. The reduced longitudinal susceptibility can be calculated either by using MFA as

$$\widetilde{\chi}_{\parallel}(T) = \begin{cases} \dfrac{\mu_{at}\beta L'}{1-\beta J_0 L'} & T \lesssim T_c, \\ \dfrac{\mu_{at} T_c}{J_0(T-T_c)} & T \gtrsim T_c, \end{cases} \tag{20}$$

where L' is the derivative of the Langevin function evaluated at $\beta J_0 m_e$, or by ASD simulations (Hinzke et al. 2000).

The first term in Eq. (15) describes the precession of magnetization vector $\mathbf{m}$ around its effective field $\mathbf{H}_{\mathrm{eff}}$ (see Fig. 3a), and the second and the third terms

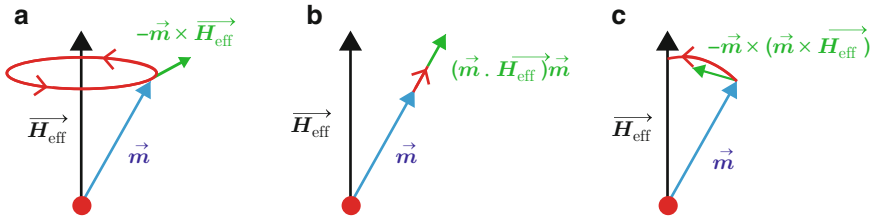

Fig. 3 Diagram illustrating the meaning of three terms in the LLB equation: (**a**) precession, (**b**) longitudinal dynamics, and (**c**) transverse dynamics. (Reprinted from Nieves 2015)

describe the longitudinal (see Fig. 3b) and the transverse (see Fig. 3c) dynamics, respectively. Comparing the LLB equation (15) with LLG equation (9), we notice that the former contains an extra term which describes the longitudinal relaxation, that is, it drives the dynamics of the magnitude of **m** giving a more accurate description of the magnetic dynamics at elevated temperatures. In particular this extra term plays a crucial role in ultrafast magnetization dynamics, i.e., at the timescale below 1 ps. At low temperatures the additional internal field in Eq. (17) is very large (since the susceptibility is very small) and keeps the magnetization length constant. Since the LLB equation contains the LLG one, it also describes the damped precession which typically takes place between 0.1 and 10 ns (see Fig. 3a).

The effective field of the LLB equation given by Eq. (17) can be also obtained as

$$\mathbf{H}_{\text{eff}}^{i} = -\frac{1}{V_i}\frac{\partial \mathcal{F}}{\partial \mathbf{M}_i}, \tag{21}$$

where $\mathcal{F}$ is the free energy given by

$$\mathcal{F}(\mathbf{M},T) = \mathcal{F}_0 + \int_V d\mathbf{r}\{-\mathbf{M}\cdot\mathbf{H} + \frac{1}{2\chi_\perp}(M_x^2+M_y^2) + A\left(\nabla\left[\frac{\mathbf{M}}{M}\right]\right)^2 + \frac{1}{8M_e^2(T)\chi_\parallel}[M^2 - M_e^2(T)]^2\}, \tag{22}$$

where $\mathcal{F}_0$ is the equilibrium free energy in the absence of anisotropy and magnetic field, $\chi_\parallel = M_s(0)\widetilde{\chi}_\parallel$ and $\chi_\perp = M_s(0)\widetilde{\chi}_\perp$. In Kachkachi and Garanin (2001) derived this free energy in the whole temperature range using a procedure based on the MFA. Obviously close to the transition temperature, this functional is reduced to the well-known Landau-Ginzburg expression. This derivation further justifies the thermodynamic consistency of the LLB equation.

Similarly as it was done in the micromagnetic LLG equation, Garanin and Chubykalo-Fesenko (2004) included stochastic thermal fields into the LLB equation. However, Evans et al. (2012) noticed that this approach doesn't recover the Boltzmann distribution close to T_c at equilibrium. In order to solve this issue, they suggested an alternative stochastic LLB equation of the form

$$\frac{d\mathbf{m}_i}{dt} = -\gamma\left[\mathbf{m}_i \times \mathbf{H}^i_{\text{eff}}\right] + \frac{\gamma\alpha_\parallel}{m_i^2}\left(\mathbf{m}_i \cdot \mathbf{H}^i_{\text{eff}}\right)\mathbf{m}_i - \frac{\gamma\alpha_\perp}{m_i^2}\left[\mathbf{m}_i \times \left[\mathbf{m}_i \times \left(\mathbf{H}^i_{\text{eff}} + \boldsymbol{\zeta}_{i,\perp}\right)\right]\right] + \boldsymbol{\zeta}_{i,ad}, \tag{23}$$

with two thermal fields: a multiplicative transverse $\boldsymbol{\zeta}_{i,\perp}$ and an additive longitudinal $\boldsymbol{\zeta}_{i,ad}$ given by

$$\left\langle \zeta^k_{i,\perp}(0)\zeta^l_{j,\perp}(t)\right\rangle = \frac{2\gamma k_B T\left(\alpha_\perp - \alpha_\parallel\right)}{M_e(0)V_i\alpha_\perp^2}\delta_{ij}\delta_{kl}\delta(t) \tag{24}$$

$$\left\langle \zeta^k_{i,ad}(0)\zeta^l_{j,ad}(t)\right\rangle = \frac{2\gamma k_B T\alpha_\parallel}{M_e(0)V_i}\delta_{ij}\delta_{kl}\delta(t), \tag{25}$$

where i and j denote macrospin index and k and l denote the Cartesian components x, y, and z. Thus in order to describe the thermal dispersion of the magnetization trajectories, we now have a Langevin dynamics simulations based on the LLB equation. The dispersion of magnetization trajectories is very important for modeling of magnetization dynamics under the action of thermal laser pulse (Kazantseva et al. 2008a). Note that not very close to T_c the approaches of Garanin and Chubykalo-Fesenko (2004) and Evans et al. (2012) are indistinguishable.

The comparison of the macrospin LLB equation with direct ASD simulations gives a very good agreement (Chubykalo-Fesenko et al. 2006; Kazantseva et al. 2008a). Note that a typical problem of the thermal micromagnetics is the presence of finite-size effects, i.e., the dependence of the average magnetization on the discretization size. Comparatively to the LLG approach, thermal micromagnetics based on the LLB equation have these effects largely reduced (Atxitia et al. 2007). This happens due to the fact that the LLB equation forces the equilibrium solution to be M_e. However, the finite-size effects are an inherent part of the thermal micromagnetic approach and are always present (Atxitia et al. 2007). If these effects are taken into account, the agreement between the atomistic and LLB-based micromagnetics can be even better (Vogler et al. 2014, 2016).

3 The Quantum (Semiclassical) Landau-Lifshitz-Bloch Equation

The above LLB equation is based on the ASD approach. There is also a quantum derivation, which was published even earlier than the classical one by Garanin et al. (1990) and Garanin (1991). Obviously, the quantum derivation can be made for simplified models only. In the original derivation, this was done for an isolated spin interacting with a phonon bath via direct and Raman processes with the Hamiltonian presented in Fig. 4. Lately, this was also done for a spin interacting with a simple electron bath by Nieves et al. (2014) following a simple model of Koopmans et al. (2005) conceived for ultrafast magnetization dynamics.

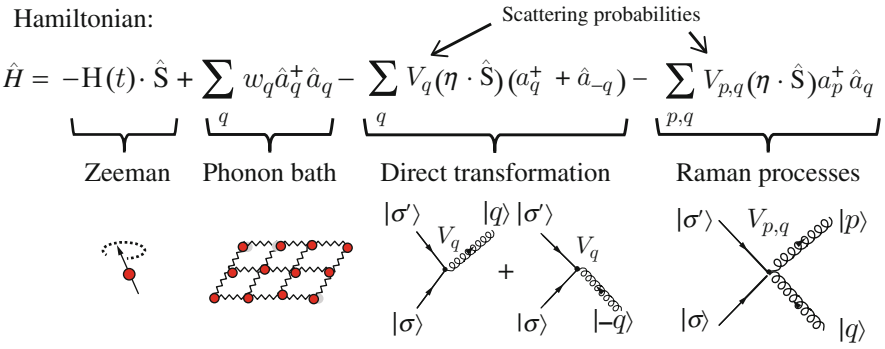

Fig. 4 The sketch of the quantum model based on the spin-phonon scattering. (Reprinted from Nieves 2015)

The derivation of the quantum LLB (qLLB) equation by Garanin (1991) is based on a standard density matrix approach (see, e.g., Blum 1981; Garanin 2012) for a system interacting weakly with a bath. The sketch for the spin-phonon model is presented in Fig. 4, and the spin-electron model can be found in Nieves et al. (2014). Namely, starting from the Schrödinger equation, one can obtain a Liouville equation for the time evolution of the density operator $\hat{\rho} = |\Psi\rangle\langle\Psi|$, where $|\Psi\rangle$ is the wave function of the whole system (spin and phonons or spin and electrons). Next, the bath is assumed to be in a quasi-equilibrium meaning that at this timescale the phonon (electron) distribution can be described by the Bose-Einstein (Fermi-Dirac) one with a defined temperature (Nieves et al. 2014) although the temperature is still slow varying in time. The temperature dynamics can be external, for example, described by the two-temperature model (Atxitia et al. 2007; Nieves and Chubykalo-Fesenko 2016; John et al. 2017; Mendil et al. 2014). Note that in the self-consistent description, the magnetization dynamics also produces a temperature dynamics and vice versa (Nieves et al. 2016).

Furthermore, the interactions with the bath are assumed to be small so that they cannot cause a significant entanglement between both systems; this allows to factorize the density operator by its spin and bath part $\hat{\rho}(t) \cong \hat{\rho}_s(t)\hat{\rho}_b^{eq}$ and average over the bath variable (Garanin 2012). The following approximations are also made: (i) the Markov or short memory approximation assuming that the spin dynamics is slower than the phonon (electron) dynamics; (ii) the secular approximation, which consists in neglecting the fast oscillating terms; (iii) as in the classical case, the interactions are taken into account in the MFA, the homogeneous part of the exchange field is considered to be much larger than all other approximations, and close to T_c the expansion $H_\mathrm{E} \simeq (J_0/\mu_\mathrm{at})(m_e + \widetilde{\chi}_\parallel h)$ is used.

The final formal form of the qLLB equation is the same as in the classical case (15), the equilibrium magnetization is defined now by the Brillouin function for the spin S: $m_e = B_S(\beta J_0 m_e)$, and the MFA longitudinal susceptibility $\widetilde{\chi}_\parallel$ follows from it at $T < T_c$ as $\widetilde{\chi}_\parallel = \mu_{at}\beta B_S'/(1 - \beta B_S' J_0)$ where $B_S'(x) = dB_S/dx$ is

evaluated at the equilibrium $B_S' = B_S'(\beta J_0 m_e)$. The parameters $\alpha_\parallel$ and $\alpha_\perp$ are different and can be conveniently expressed in a form which is suitable for the comparison with the classical LLB equation. Below T_c the damping parameters are written as

$$\alpha_\parallel = \lambda \frac{2T}{3T_c} \frac{2q_s}{\sinh(2q_s)} \tag{26}$$

$$\alpha_\perp = \lambda \left[\frac{\tanh(q_s)}{q_s} - \frac{2T}{3T_c} \left(1 - \frac{K_1}{2K_2} \right) \right], \tag{27}$$

where $q_s = 3T_c m_e/(2(S+1)T)$ and

$$\lambda = K_2 \frac{(S+1)}{S} \frac{\mu_{at}}{\gamma k_B T}. \tag{28}$$

has the sense of atomistic damping (coupling to the bath) parameter. The parameters K_1 and K_2 are related to the microscopic scattering probabilities (see Nieves et al. 2014).

Below T_c the effective field used in Eq. (15) is given by Eq. (17). Above T_c we also rewrite the effective field in terms of the longitudinal susceptibility at $T > T_c$, i.e., $\tilde{\chi}_\parallel = \mu T_c/[J_0(T - T_c)]$, and the field reads as

$$\mathbf{H}_{\text{eff}} = -\frac{1}{\tilde{\chi}_\parallel} \left(1 + \frac{3T_c m^2}{5A_s(T - T_c)} \right) \mathbf{m} + \mathbf{h} \ , \ \frac{T_c}{T - T_c} \gg 1, \tag{29}$$

where $A_s = 2(S+1)^2/([S+1]^2 + S^2)$ and $\mathbf{h}$ contains all other fields (Zeeman, anisotropy, (external) inter-macrospin exchange, and magnetostatic). Note that although $\widetilde{\chi}_\parallel$ is divergent at T_c as it corresponds to the second-order phase transition, the internal exchange field is the same for any $T_c - \varepsilon$ and $T_c + \varepsilon$ insuring that under the integration of the LLB equation, $\mathbf{m}(t)$ rests continuous through the critical point. In the region just above T_c, $q_s = 0$ and $K_1 \cong K_2$, so that the damping parameters become approximately the same and equal to the one presented in Eq. (16), where the dependence on the spin value S is included implicitly through λ (see Eq. (28)).

In the special case with $S = 1/2$ and pure longitudinal dynamics, the qLLB equation is reduced (see details in Nieves et al. 2014) to the so-called self-consistent Bloch equation (see Xu and Zhang 2012)

$$\frac{d\mathbf{m}}{\mathrm{d}t} = -\gamma \mathbf{m} \times \mathbf{h} - \frac{\mathbf{m} - \mathbf{m}_0}{\tau_s}, \tag{30}$$

where $\mathbf{m}_0 = B_{1/2}(\xi)\boldsymbol{\xi}/\xi$ and $\tau_s = 1/K_2$ the spin relaxation time. This equation may be further simplified taking into account that the exchange field is large in which case it is reduced to

$$\frac{\mathrm{d}m}{\mathrm{d}t} = \frac{m}{\tau_s}\left[1 - m\coth\left(\frac{mT_c}{T}\right)\right]. \tag{31}$$

The above equation was used as a part of the so-called three-temperature model (M3TM) by Koopmans et al. (2010), in which τ_s is related to the Elliott-Yafet scattering probability.

4 The Two-Sublattice Landau-Lifshitz-Bloch Equation

For the treatment of a two-sublattice ferro- or ferrimagnet by Atxitia et al. (2012), two Eq. (12) are written for each sublattice separately, and the mean field contains inter- and intra-sublattice contributions. For the disordered case with different concentrations of the species (such as the case of Gd_xCo_{1-x}, see Fig. 5), the MFA field reads:

$$\mathbf{H}_v^{\mathrm{MFA}} = \frac{J_{0,v}}{\mu_v}\mathbf{m}_v + \frac{J_{0,v\kappa}}{\mu_v}\mathbf{m}_\kappa + \mathbf{h}_v, \tag{32}$$

where $J_{0,v} = x_v z J_{vv}$, $J_{0,v\kappa} = x_\kappa z J_{v\kappa}$; z is the number of nearest neighbors in the ordered lattice; J_{vv} and $J_{v\kappa}$ are the Heisenberg intra- and intersublattice exchange interaction parameters; x_v and $x_\kappa = 1 - x_v$ are the concentrations of the sublattices v and κ, respectively; and $\mathbf{h}_v$ contains the external applied and the anisotropy fields acting on the sublattice v. With the same approximations as in the case of the classical one sublattice LLB equation, one arrives at two coupled LLB equations of the form Eq. (15) for each sublattice, where the effective field is given by

$$\begin{aligned}\mathbf{H}_{\mathrm{eff},v} = \mathbf{H} + \mathbf{H}_{\mathrm{A},v} + \frac{J_{0,v\kappa}}{\mu_v}\mathbf{\Pi}_\kappa \\ - \left[\frac{1}{\Lambda_{vv}}\left(m_v - m_{e,v}\right) - \frac{1}{\Lambda_{v\kappa}}\left(|\tau_\kappa| - |\tau_{e,\kappa}|\right)\right]\frac{\mathbf{m}_v}{m_v},\end{aligned} \tag{33}$$

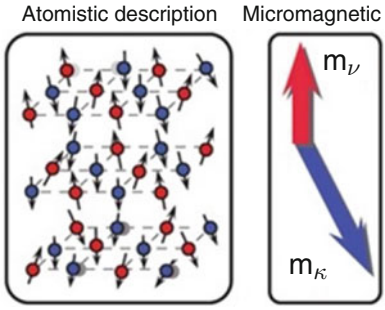

Fig. 5 Sketch of a disordered magnetic alloy from the point of view of the atomistic model (left panel) and the micromagnetic LLB model (right panel). (Reprinted from Atxitia et al. 2012)

where $\mathbf{H}_{\mathrm{A},v}$ is the anisotropy field, $\mathbf{H}$ is the applied field, $\mathbf{\Pi}_\kappa = -[\mathbf{m}_v \times [\mathbf{m}_v \times \mathbf{m}_\kappa]]/m_v^2$, $\tau_v = (\mathbf{m}_v \cdot \mathbf{m}_\kappa)/m_\kappa$, $\tau_{e,v} = (\mathbf{m}_{e,v} \cdot \mathbf{m}_{e,\kappa})/m_{e,\kappa}$, and

$$\Lambda_{vv}^{-1} = \frac{1}{\widetilde{\chi}_{v,||}}\left(1 + \frac{J_{0,v\kappa}}{\mu_v}\widetilde{\chi}_{\kappa,||}\right), \quad \Lambda_{v\kappa}^{-1} = \frac{|J_{0,v\kappa}|}{\mu_v}. \tag{34}$$

The longitudinal susceptibility can be calculated in the MFA as in Atxitia et al. (2012)

$$\widetilde{\chi}_{v,||} = \frac{\mu_\kappa \beta L'_v J_{0,v\kappa} \beta L'_\kappa + \mu_v \beta L'_v \left(1 - J_{0,\kappa}\beta L'_\kappa\right)}{\left(1 - J_{0,v}\beta L'_v\right)\left(1 - J_{0,\kappa}\beta L'_\kappa\right) - J_{0,\kappa v}\beta L'_v J_{0,v\kappa}\beta L'_\kappa}, \tag{35}$$

where $L'_v = L'(\xi_{e,v})$ with $\xi_{e,v} = \beta(J_{0,v}m_{e,v} + |J_{0,v\kappa}|m_{e,\kappa})$. The damping parameters are

$$\alpha_{\|}^v = \frac{2\lambda_v}{\beta \widetilde{J}_{0,v,e}}, \quad \alpha_{\perp}^v = \lambda_v\left(1 - \frac{1}{\beta \widetilde{J}_{0,v,e}}\right), \tag{36}$$

where $\widetilde{J}_{0,v,e} = J_{0,v} + |J_{0,v\kappa}|(m_{e,\kappa}/m_{e,v})$. Note that all the expressions above are the same for two-sublattice ferrimagnetic and ferromagnetic alloys.

The quantum case only differs by the damping parameters which now have the forms (see Nieves 2015):

$$\alpha_{\|}^v = \frac{2\lambda_v}{\beta \tilde{J}_{0,v,e}}\left(\frac{S_v}{S_v + 1}\right)\frac{2q_v}{\sinh(2q_v)}, \tag{37}$$

$$\alpha_{\perp}^v = \lambda_v\left[\frac{\tanh(q_v)}{q_v} - \frac{2S_v}{(S_v + 1)\beta \tilde{J}_{0,v,e}}\left(1 - \frac{K_{1,v}}{2K_{2,v}}\right)\right], \tag{38}$$

where $q_v = (\beta \tilde{J}_{0,v,e} m_{e,v})/(2S_v)$ and $\lambda_v = [\beta \mu_v K_{2,v}(S_v + 1)]/[\gamma_v S_v]$.

In the equations above the longitudinal susceptibility $\widetilde{\chi}_{v,\|}$ should be evaluated in MFA using the Brillouin function.

Taking the limits $S_v \to \infty$ and $S_\kappa \to \infty$ in the quantum version, we arrive to the classical LLB equation for disordered magnetic alloys. On the other hand, if we take the limit $x_\kappa \to 0$ (i.e., the impurities are removed), then we obtain the qLLB equation for a ferromagnet. Very recently, Vogler et al. (2018) incorporated stochastic fluctuations to the classical two-sublattice LLB.

4.1 The Relaxation Rates

The main difference of the high-temperature micromagnetics based on the LLB equation and the conventional micromagnetics is the temperature-dependent relaxation. It is defined by the two main characteristic times, obtained by the linearization. These are the longitudinal relaxation time

$$\tau_{\parallel} = \frac{\widetilde{\chi}_{\parallel}}{\gamma \alpha_{\parallel}}, \tag{39}$$

which defines the speed of the change of the magnetization length and the transverse relaxation time $\tau_{\perp}$, i.e., the characteristic time taken by the transverse component of magnetization to relax to the effective field **h** including the external field and the anisotropy contributions

$$\tau_{\perp} = \frac{\gamma\, h\, m_e}{\alpha_{\perp}}. \tag{40}$$

The corresponding transverse relaxation below T_c may be put in the more common form of the macroscopic LLG equation. For this instead of the normalization of magnetization to the total spin polarization, one should use its normalization to the saturation magnetization value, i.e., $M_e(T)$. The resulting equation is the same LLB one but with a different damping parameters, called here α_{LLG}.

$$\alpha_{\mathrm{LLG}} = \frac{\alpha_{\perp}}{m_e}. \tag{41}$$

Note that while both $\alpha_{\parallel}$ and $\alpha_{\perp}$ are continuous through T_c, $\tau_{||}$ and α_{LLG} diverge at T_c, corresponding to the critical behavior at the phase transition. At the same time the perpendicular relaxation time goes to zero which constitutes one of the main differences between the LLG and the LLB dynamics.

The most important manifestation of the high-temperature dynamics is the longitudinal relaxation time. It will show itself only close to the phase transition due to the fact that at relatively low temperatures the longitudinal susceptibility is small. At T_c the susceptibility diverges as well as the longitudinal relaxation time. This divergence is only visible very close to T_c so that for practical reasons the longitudinal timescale is still at femtosecond scale for $T/T_c = 0.9$. However, this timescale is now accessible with the ultrafast magnetization dynamics exited by fs laser or THz radiation.

An example of the temperature dependence of the longitudinal relaxation time is presented in Fig. 6. It has the following asymptotic behavior:

$$\tau_{||} \cong \frac{\mu_{at}}{2\gamma\lambda k_B T_c}\frac{S+1}{S}\begin{cases} \frac{T_c}{TS} & T \ll \min(T_c, \frac{T_c}{S}), \\ \frac{1}{3}\left[1+\left(\frac{S}{S+1}\right)\frac{T}{T_c}\right] & \frac{T_c}{S} \ll T \ll T_c, \\ \frac{T_c}{2(T_c-T)} & \frac{T_c}{T_c-T} \gg 1, \\ \frac{T_c}{T-T_c} & \frac{T_c}{T-T_c} \gg 1. \end{cases} \tag{42}$$

Note that its behavior is in agreement with the well-known relation, proposed by Koopmans et al. (2010), that the ultrafast demagnetization time scales with the ratio μ_{at}/T_c and proposed by Kazantseva et al. (2008b) and Ostler et al. (2012) that it scales as a ratio μ_{at}/λ . As was pointed out elsewhere by Atxitia and Chubykalo-Fesenko (2011) and Atxitia et al. (2014), the complete expression involves the

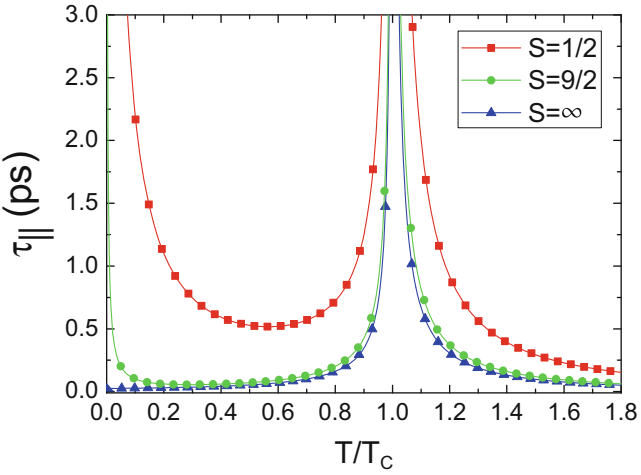

Fig. 6 Longitudinal relaxation time (Eq. (39)) versus temperature using constant $\lambda = 0.02$, $T_c = 650$ K, and $\mu_{at} = 0.5\mu_B$ in the three spin cases with $S = 1/2$, $S = 9/2$, and $S = \infty$. The case $S = \infty$ is done by taking the limit $S \to \infty$ in Eq. (39), which is equivalent to the classical LLB equation. (Reprinted from Nieves et al. 2014)

combination of both. The two last lines in Eq. (42) describe the effect of the critical slowing down near the critical temperature. Note that the relaxation time is twice large above T_c than below it. Furthermore, the relaxation time decreases with the increase of the quantum number S. This is due to the fact that for larger S one increases the number of scattering possibilities. Furthermore, there is also an increase of the longitudinal relaxation time for low temperatures, visible especially for $S = 1/2$. This is due to the well-known fact of the freezing of fluctuations at low temperature in the quantum case and is reflected also in the fact that the perpendicular damping parameter goes to zero in the quantum case (see Eq. (27)), while it tends to a constant value in the classical case. In any case, there is an additional temperature dependence not considered above due to the fact that $\lambda(T)$ is a function of temperature itself since it contains the scattering probabilities. This dependence is specific for the scattering mechanism (see Nieves et al. 2014, Nieves 2015).

While in the LLB equation we use the longitudinal susceptibility at zero field (diverging at T_c), the resulting susceptibility at constant field does not diverge. In Fig. 7 we present the longitudinal relaxation time as a function of the temperature in constant applied field for the two limiting cases $S = 1/2$ and $S = \infty$. The longitudinal relaxation time was evaluated by direct integration of the qLLB equation with initial conditions $m_0 - m_e = 0.1m_e$. The longitudinal relaxation time for $S = 1/2$ is smaller in the classical case than for the quantum one, and, as expected, the maximum is displaced for larger values at larger fields.

For the two-sublattice case, it is also possible to analyze the relaxation rates of the two sublattices. However, the equations are coupled and the situation depends

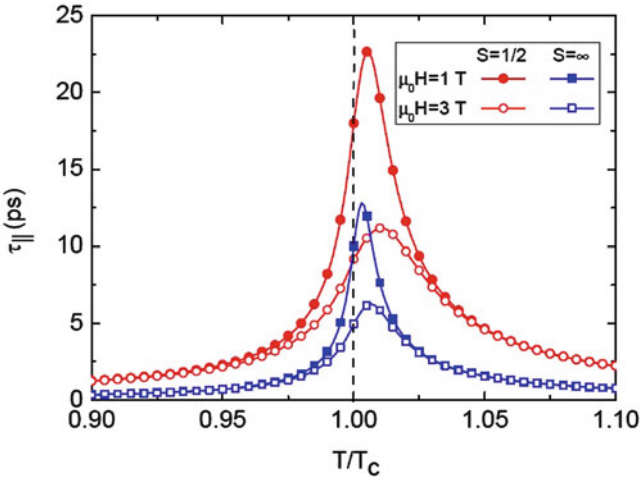

Fig. 7 The in-field longitudinal relaxation time calculated via direct integration of the qLLB equation with small deviation from the equilibrium. The following parameters are used $T_c = 650\,\mathrm{K}$, $\mu_{\mathrm{at}} = 0.5\mu_B$, $\lambda = 0.02$, and zero anisotropy constant. (Reprinted from Nieves et al. 2014)

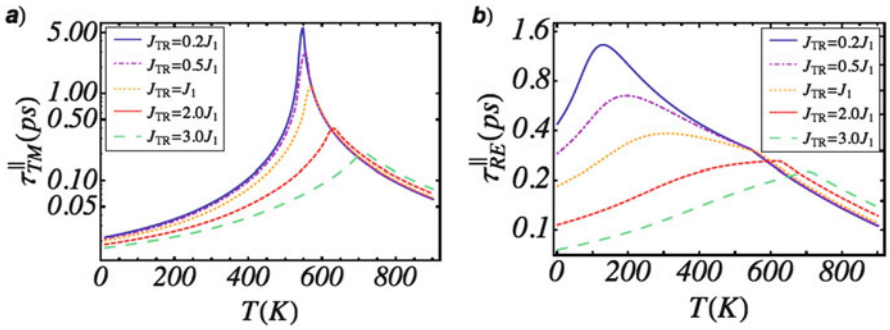

Fig. 8 Longitudinal relaxation time of the (**a**) transition metal (TM), strong intersublattice exchange and (**b**) rare earth (RE), weak intersublattice exchange, evaluated for the $Gd_{0.25}Fe_{0.75}$ compound and different intersublattice strengths J_{TR}. The parameter J_1 corresponds to a typical (relatively weak) intersublattice strength of this material (see Suarez et al. 2015 and Ostler et al. 2011 for the values). (Reprinted from Suarez et al. 2015)

strongly on the coupling strength. Typically the divergence of the longitudinal relaxation time is suppressed by interactions (as in the case of the external field), and individual longitudinal relaxation times simply have maximum at different critical temperatures for each sublattice. An example of the longitudinal relaxation time for different intersublattice exchange strengths is presented in Fig. 8. In weakly coupled ferrimagnets, only the material with the largest exchange value slows down at the common Curie temperature (see Suarez et al. 2015).

If the coupling is not very strong and for relatively low temperatures, we can estimate the longitudinal relaxation time as defined by the exchange field acting on each sublattice as

$$\tau_v^{||} \approx \frac{1}{2\gamma_v \lambda_v m_{v,e} H_{v,e}^{ex}}, \tag{43}$$

where

$$H_{v,e}^{ex} = \frac{\widetilde{J}_{0,v,e}}{\mu_v} m_{e,v}, \tag{44}$$

is the homogeneous exchange field evaluated at the equilibrium. Note that in this approximation, the relaxation time is independent on the sign of the coupling between sublattices (ferro or antiferro).

Interestingly that varying the initial temperature, the demagnetization speed of the initially slower material may become faster than that of the high-speed material. For example, Gd in GdFe may become faster than Fe at high initial temperatures (Atxitia et al. 2014). The temperatures at which the longitudinal relaxation times are maximum coincide for each sublattice in the case of strongly coupled alloys.

The extension of the two-sublattice LLB above the Curie temperature can be found in Nieves et al. (2015) and Nieves (2015). Here the longitudinal and the transverse damping parameters become the same and defined by the formula (Eq. (16)) for each sublattice.

5 Examples of Modeling Magnetization Dynamics Close to the Phase Transition

The main difference of the LLG and LLB magnetization dynamics is the presence of the longitudinal relaxation. This relaxation manifests itself close to the Curie temperature only and especially at picosecond-femtosecond timescale. In fact, close to this temperature, the magnetization can be switched by a so-called linear reversal, i.e., when the macroscopic magnetization changes its length instead of rotating the magnetization vector as it happens at low temperatures. In the intermediate region the reversal is so-called elliptical, i.e., the magnetization vector rotates together with the change of its magnitude. For the analysis of elliptical and linear reversal within the LLB model, see Kazantseva et al. (2009). The high-temperature magnetization dynamics close to T_c is also characterized by the presence of the linear domain walls in which the magnetization changes its length rather than rotates (see, e.g., Hinzke et al. 2007).

To illustrate the appearance and importance of linear magnetization reversal path, we present in Fig. 9 the modeling results for the magnetization reversal time versus temperature for a magnetic nanoparticle with $S = 1/2$ (pure quantum case) and $S = \infty$ (classical case) under applied field $\mu_0 H_z = -1T$ for two different initial

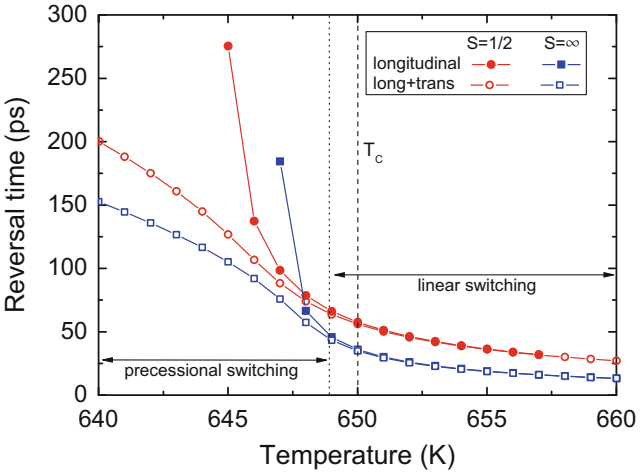

Fig. 9 Reversal time versus temperature for a magnetic nanoparticle with magnetic moment $\mu = 0.5\mu_B$ (μ_B is the Bohr magneton), $T_c = 650\,\mathrm{K}$, and the coupling to the bath parameter $\lambda = 0.02$ under applied field $\mu_0 H_z = -1T$ modeled with the LLB equation with $S = 1/2$ and $S = \infty$. In the pure longitudinal dynamics, the initial magnetization is set to $\mathbf{m} = (0, 0, 0.2)$, and in the longitudinal plus transverse dynamics, the initial magnetization is set to $\mathbf{m} = (0.05, 0, 0.2)$. (Reprinted from Nieves et al. 2014)

conditions: (i) pure longitudinal dynamics where we put the initial magnetization of nanoparticle parallel to the field so that it cannot precess and (ii) longitudinal plus transverse dynamics where the initial magnetization is slightly tilted from the field axis. We define the reversal time as time elapsed between the initial state and the instant of time at which the magnetization begins to reverse its direction, i.e., crosses $m_z = 0$ point. One can observe that slightly below and above T_c, the magnetization reversal becomes completely linear, i.e., occurs by a pure change of the magnetization magnitude. However, at 5 degrees from T_c, the path is elliptical and at 10 degrees, it is completely precessional.

The longitudinal relaxation especially manifests itself in the laser-induced magnetization dynamics which recently has become an essential part of the novel field of opto-magnetism (Kimel et al. 2007; Kirilyuk et al. 2010). Indeed the timescale in these experiments goes down to the femtosecond range, and the energies are such that the electronic temperature often exceeds the Curie temperature of the materials. One of the main acting mechanisms has a pure heat origin (see Ostler et al. 2012), and during the femtosecond timescale, the exchange interaction energy is probed. The modeling of the ultrafast laser-induced magnetization dynamics based on the LLB equation has been successfully performed in Ni (Atxitia et al. 2010a), in FeNi (Hinzke et al. 2015), Gd (Sultan et al. 2012), and FePt (Mendil et al. 2014) with a very good agreement with experiment. For this purpose the LLB equation is coupled with the electronic temperature of the two-temperature model assuming the electron scattering mechanism.

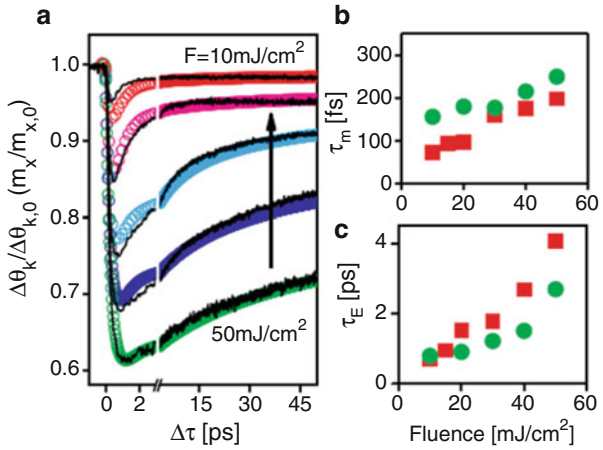

Fig. 10 (left panel) The measured Kerr angle rotation (solid line) and the modeled magnetization dynamics (circles) for various laser fluencies F on Ni. The right panels represent experimental (circles) and modeled (squares) timescales for demagnetization τ_m and recovery τ_E. (Reprinted from Atxitia 2012)

The main consequence of the longitudinal relaxation is the slowing down of the first laser-induced demagnetization timescale. An example of this is illustrated in Fig. 10 where we present a comparison between the experiment performed in Atxitia et al. (2010a) on Ni and the micromagnetic modeling based on the LLB equation. The right panels represent the behavior of the demagnetization τ_m and the recovery τ_E times as a function of the laser fluency. The slowing down of the demagnetization timescale is the consequence of the slowing down of the longitudinal relaxation time, while the slowing down of the recovery timescale is the consequence of the electronic temperature dynamics. The comparison of the experimental measurements with the modeling based on the LLB has allowed to conclude the pure thermal origin of the laser-induced demagnetization. This was later confirmed by atomistic modeling and experiments on different FeCoGd thin films and dots by Ostler et al. (2012).

Another prominent example is the magnetization dynamics measured and modeled in FePt thin film with a linearly polarized laser pulse by Mendil et al. (2014). Here as the laser pulse intensity increases and the quasi-equilibrium electron temperature approaches the Curie temperature, the slowing down of the demagnetization time of FePt in the picosecond timescale is observed experimentally and in modeling. At large pulse intensity the quasi-equilibrium electron temperature stays near T_c, and the recovery does not take place in the 100 ps timescale. The result of the modeling is presented in Fig. 11. The experiment and LLB-based modeling with circularly polarized laser pulse can be found in John et al. (2017). The circular polarized light produces an additional effect based on the inverse Faraday one (Hertel 2005; Vahaplar et al. 2012; Battiato et al. 2014). This suppresses the slowing

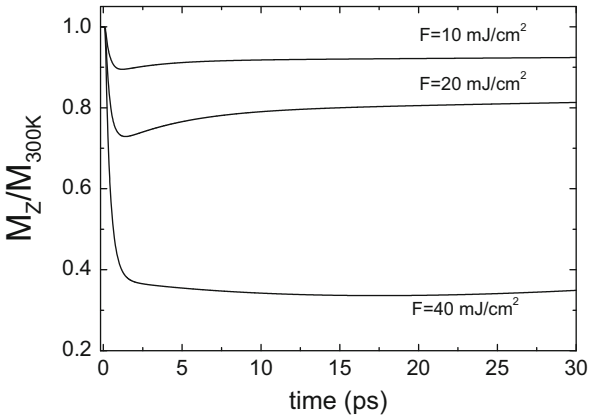

Fig. 11 Magnetization dynamics in FePt under the linearly polarized laser pulse obtained by the integration of the qLLB equation with $S = 3/2$ coupled with the two-temperature model with the parameters from Mendil et al. (2014), Nieves (2015) and for several laser intensities measured in fluence F. (Reprinted from Nieves 2015)

down and makes the reversal probabilities from up to down and from down to up to become non-equal. A similar effect is produced treating the inverse Faraday effects as an additional short timescale field (Nieves and Chubykalo-Fesenko 2016). In John et al. (2017) the reversal probabilities were modeled within the multiscale approach based on the DFT calculations, LLB approach, and the rate equations. The modeling results explained the recently observed by Lambert et al. (2014) switching of FePt granular media by circularly polarized pulses.

The two-sublattice LLB approach was successfully used to explain the temperature dependence of the frequencies and damping parameter of ferro- and antiferromagnetic modes in GdFe ferrimagnet (Schlickeiser et al. 2012) and to explain the different demagnetization speeds in Fe and Ni in permalloy (Hinzke et al. 2015).

Furthermore the LLB approach is currently extensively used as a framework for modeling of heat-assisted magnetic recording (McDaniel 2012; Vogler et al. 2014, 2016). It is especially useful for a coarse-grained modeling when one magnetic grain can be represented as the LLB macrospin (Vogler et al. 2014, 2016).

Recently several extensions of the LLB model also appeared, to mention the introduction of the spin-torque effects into the LLB model by Schieback et al. (2009) or Janda et al. (2017), of the colored noise (Atxitia 2012) or the self-consistent modeling of magnetization and temperature dynamics (Nieves et al. 2016) useful for modeling of magnetocaloric effect and magnetic hyperthermia.

6 Conclusions

The LLB approach is a valuable micromagnetic framework to model magnetization dynamics close to T_c and in general where rapid temperature changes appear. First, it correctly reproduces the temperature dependence of relaxational parameters and is in agreement with atomistic modeling. Second, it has proved its viability in modeling of several important research areas such as the heat-assisted magnetic

recording, spin caloritronics, and ultrafast laser-induced magnetization dynamics and was validated via the experimental measurements. It is an important part of the multiscale framework, especially when the model should include the temperature effects. The introduction of the quantum LLB equation allows one to pass directly from ab initio modeling to the micromagnetic one without going through the atomistic part and avoiding the classical temperature dependencies of the micromagnetic parameters as opposed to the more correct quantum dependencies. This, however, needs future investigation on the relevant scattering mechanisms and their spin-flip probabilities. The generalization of the LLB equation for the case of alloys allows one to describe separately the dynamics of each species, in agreement with experimental predictions that these dynamics are different on the ultrashort timescale.

Acknowledgments This work was supported by the Spanish Ministry of Economy and Competitiveness under the project FIS201678591-C3-3-R. P.N. acknowledges support from EU Horizon 2020 Framework Programme for Research and Innovation under Grant Agreement No. 686056, NOVAMAG.

References

Asselin P, Evans RFL, Barker J, Chantrell RW, Yanes R, Chubykalo-Fesenko O, Hinzke D, Nowak U (2010) Constrained Monte Carlo method and calculation of the temperature dependence of magnetic anisotropy. Phys Rev B 82:054415

Atxitia U (2012) Modeling of ultrafast laser-induced magnetization dynamics within the Landau-Lifshitz-Bloch approach. Ph.D. thesis, Instituto de Ciencia de Materiales de Madrid (ICMM) – Universidad Autónoma de Madrid

Atxitia U, Chubykalo-Fesenko O (2011) Ultrafast magnetization dynamics rates within the Landau-Lifshitz-Bloch model. Phys Rev B 84:144414

Atxitia U, Chubykalo-Fesenko O, Kazantseva N, Hinzke D, Nowak U, Chantrell RW (2007) LLB-micromagnetic modelling of laser-induced magnetisation dynamics. Appl Phys Lett 91:232507

Atxitia U, Chubykalo-Fesenko O, Walowski J, Mann A, Münzenberg M (2010a) Evidence for thermal mechanisms in laser-induced femtosecond spin dynamics. Phys Rev B 81:174401

Atxitia U, Hinzke D, Chubykalo-Fesenko O, Nowak U, Kachkachi H, Mryasov ON, Evans RF, Chantrell RW (2010b) Multiscale modeling of magnetic materials: temperature dependence of the exchange stiffness. Phys Rev B 82:134440

Atxitia U, Nieves P, Chubykalo-Fesenko O (2012) Landau-Lifshitz-Bloch equation for ferrimagnetic materials. Phys Rev B 86:104414

Atxitia U, Barker J, Chantrell RW, Chubykalo-Fesenko O (2014) Controlling the polarity of the transient ferromagneticlike state in ferrimagnets. Phys Rev B 89:224421

Atxitia U, Hinzke D, Nowak U (2016) Fundamentals and applications of the Landau-Lifshitz-Bloch equation. J Phys D Appl Phys 50:033003

Battiato M, Barbalinardo G, Oppeneer PM (2014) Phys Rev B 89:014413

Beaurepaire E, Merle JC, Daunois A, Bigot JY (1996) Ultrafast spins dynamics in ferromagnetic nickel. Phys Rev Lett 76:4250

Bloch F (1946) Nuclear induction. Phys Rev 70:460

Blum K (1981) Density matrix theory and applications. Plenum Press, New York

Brown WF (1963a) Micromagnetics. Wiley, New York

Brown WF (1963b) Thermal fluctuations of a single-domain particle. Phys Rev 130:1677

Chantrell RW, Wongsam M, Schrefl T, Fidler J (2001) Micromagnetics I: basic principles. In: Buschow KHJ, Cahn RW, Flemings MC, Ilschner B, Kramer EJ, Mahajan S (eds) Encyclopedia of materials: science and technology. Elsevier, Amsterdam

Chubykalo O, Hannay JD, Wongsam MA, Chantrell RW, González JM (2002) Langevin dynamic simulation of spin waves in a micromagnetic model. Phys Rev B 65:184428

Chubykalo O, Smirnov-Rueda R, Wongsam MA, Chantrell RW, Nowak U, González JM (2003) Brownian dynamics approach to interacting magnetic moments. J Magn Magn Mat 266:28

Chubykalo-Fesenko O, Nowak U, Chantrell RW, Garanin D (2006) Dynamic approach for micromagnetics close to the Curie temperature. Phys Rev B 74:094436

Coey J (2009) Magnetism and magnetic materials. Cambridge University Press, New York

Eriksson O, Bergman A, Bergqvist L, Hellsvik J (2017) Atomistic spin dynamics foundations and applications. Oxford University Press, New York

Evans RFL, Hinzke D, Atxitia U, Nowak U, Chantrell RW, Chubykalo-Fesenko O (2012) Stochastic form of the Landau-Lifshitz-Bloch equation. Phys Rev B 85:014433

Evans RFL, Fan WJ, Chureemart P, Ostler TA, Ellis MOA, Chantrell RW (2014) Atomistic spin model simulations of magnetic nanomaterials. J Phys Cond Mat 26:103202

Fidler J, Schrefl T (2000) Micromagnetic modelling—the current state of the art. J Phys D Appl Phys 33:R135

Garanin DA (1991) Generalized equation of motion for a ferromagnet. Phys A 172:470

Garanin DA (1997) Fokker-Planck and Landau-Lifshitz-Bloch equation for classical ferromagnets. Phys Rev B 55:3050

Garanin DA (2012) Density matrix equation for a bathed small system and its application to molecular magnets. Adv Chem Phys 147:213

Garanin DA, Chubykalo-Fesenko O (2004) Thermal fluctuations and longitudinal relaxation of single-domain magnetic particles at elevated temperatures. Phys Rev B 70:212409

Garanin DA, Ishtchenko VV, Panina LV (1990) Dynamics of an ensemble of single-domain magnetic particles. Theor Math Phys 82:169

García-Palacios JL, Lázaro FJ (1998) Langevin-dynamics study of the dynamical properties of small magnetic particles. Phys Rev B 58:14937

Gilbert T (2004) A phenomenological theory of damping in ferromagnetic materials. IEEE Trans Magn 40:6

Greaves SJ, Muraoka H, Kanai Y (2015) Modelling of heat assisted magnetic recording with the landau-lifshitz-bloch equation and brillouin functions. J Appl Phys 117:17C505

Grinstein G, Koch RH (2003) Coarse graining in micromagnetics. Phys Rev Lett 90:207201

Hertel R (2005) Theory of the inverse faraday effect in metals. J Magn Magn Mater 202:L1–L4

Hinzke D, Nowak U (2011) Domain wall motion by the magnonic spin Seebeck effect. Phys Rev Lett 107:027205

Hinzke D, Nowak U, Garanin DA (2000) Uniform susceptibility of classical antiferromagnets in one and two dimensions in a magnetic field. Euro Phys J B 16:435

Hinzke D, Nowak U, Mryasov ON, Chantrell RW (2007) Orientation and temperature dependence of domain wall properties in FePt. Appl Phys Lett 90:082507

Hinzke D, Atxitia U, Carva K, Nieves P, Fesenko-Chubykalo O, Oppeneer P, Nowak U (2015) Multiscale modeling of ultrafast element specific magnetization dynamics of ferromagnetic alloys. Phys Rev B 92:054412

Janda T, Roy P, Otxoa R, Soban Z, Ramsay A, Irvine A, Trojanek F, Surynek M, Campion R, Gallagher B, Jungwirth T, Nemec P, Wunderlich J (2017) Inertial displacement of a domain wall excited by ultra-short circularly polarized laser pulses. Nat Commun 8:15226

John R, Berrita M, Hinzke D, Muller C, Santos T, Ulrichs H, Nieves P, Mondal R, Walowski J, Chubykalo-Fesenko O, McCord J, Oppenneer P, Nowak U, Muzenberg M (2017) Magnetization switching of FePt nanoparticle recording medium by femtosecond laser pulses. Sci Rep 7:4114

Kachkachi H, Garanin D (2001) Magnetic free energy at elevated temperatures and hysteresis of magnetic particles. Phys A 291:485–500

Kazantseva N (2008) Dynamic response of the magnetisation to picosecond heat pulses. Ph.D. thesis, University of York

Kazantseva N, Hinzke D, Nowak U, Chantrell RW, Chubykalo-Fesenko O (2007) Atomistic models of ultrafast reversal. Phys Stat Sol 244:4389

Kazantseva N, Hinzke D, Nowak U, Chantrell RW, Atxitia U, Chubykalo-Fesenko O (2008a) Towards multiscale modelling of magnetic materials: simulations of FePt. Phys Rev B 77:184428

Kazantseva N, Nowak U, Chantrell RW, Hohlfeld J, Rebei A (2008b) Slow recovery of the magnetisation after a sub-picosecond heat-pulse. Europhys Lett 81:27004

Kazantseva N, Hinzke D, Chantrell R, Nowak U (2009) Linear and elliptical magnetization reversal close to the curie temperature. Europhys Lett 86:27006

Kimel AV, Kirilyuk A, Rasing T (2007) Femptosecond opto-magnetism: ultrafast laser manipulation. Laser Photonics Rev 1:275–287

Kirilyuk A, Kimel AV, Rasing T (2010) Ultrafast optical manipulation of magnetic order. Rev Mod Phys 82:2731

Koopmans B, Ruigrok JJM, Longa FD, de Jonge WJM (2005) Unifying ultrafast magnetization dynamics. Phys Rev Lett 95:267207

Koopmans B, Malinowski G, Longa FD, Steiauf D, Fähnle M, Roth T, Cinchetti M, Aeschlimann M (2010) Explaining the paradoxical diversity of ultrafast laser-induced demagnetization. Nat Mat 9:259–265

Lambert CH, Mangin S, Varaprasad BSDCS, Takahashi YK, Hehn M, Cinchetti M, Malinowski G, Hono K, Fainman Y, Aeschlimann M, Fullerton EE (2014) All-optical control of ferromagnetic thin films and nanostructures. Science 345:1337

Landau DL, Lifshitz E (1935) On the theory of the dispersion of magnetic permeability in ferromagnetic bodies. Phys Z Sowjetunion 8:153

Lyberatos A, Chantrell RW (1993) Thermal fluctuations in a pair of magnetostatistically coupled particles. J Appl Phys 73:6501

McDaniel TW (2012) Application of Landau-Lifshitz-Bloch dynamics to grain switching in heat-assisted magnetic recording. J Appl Phys 112:013914

Mendil J, Nieves P, Chubykalo-Fesenko O, Walowski J, Santos T, Pisana S, Münzenberg M (2014) Resolving the role of femtosecond heated electrons in ultrafast spin dynamics. Sci Rep 4:3980

Moreno R, Evans R, Khmelevskyi S, Munoz M, Chantrell R, Chubykalo-Fesenko O (2016) Temperature-dependent exchange stiffness and domain wall width in Co. Phys Rev B 94:104433

Nakatani Y, Uesaka Y, Hayashi N, Fukushima H (1997) Computer simulation of thermal fluctuation of fine particle magnetization based on Langevin equation. J Magn Magn Mat 168:347

Nieves P (2015) Micromagnetic models for high-temperature magnetization dynamics. Ph.D. thesis, Instituto de Ciencia de Materiales de Madrid (ICMM) – Universidad Autónoma de Madrid

Nieves P, Chubykalo-Fesenko O (2016) Modeling of ultrafast heat- and field-assisted magnetization dynamics in FePt. Phys Rev Appl 5:014006

Nieves P, Serantes D, Atxitia U, Chubykalo-Fesenko O (2014) The quantum Landau-Lifshitz-Bloch equation and its comparison with the classical case. Phys Rev B 90:104428

Nieves P, Atxitia U, Chantrell RW, Chubykalo-Fesenko O (2015) The classical two sublattice Landau-Lifshitz-Bloch equation at all temperatures. Low Temp Phys 41:949

Nieves P, Serantes D, Chubykalo-Fesenko O (2016) Self-consistent description of spin-phonon dynamics in ferromagnets. Phys Rev B 94:014409

Nieves P, Arapan S, Schrefl T, Cuesta-Lopez S (2017) Atomistic spin dynamics simulations of the MnAl τ-phase and its antiphase boundary. Phys Rev B 96:224411

Ostler TA, Evans RFL, Chantrell RW, Atxitia U, Chubykalo-Fesenko O, Radu I, Abrudan R, Radu F, Tsukamoto A, Itoh A, Kirilyuk A, Rasing T, Kimel A (2011) Crystallographically amorphous ferrimagnetic alloys: comparing a localized atomistic spin model with experiments. Phys Rev B 84:024407

Ostler T, Barker J, Evans R, Chantrell R, Atxitia U, Chubykalo-Fesenko O, Moussaoui SE, Guyader LL, Mengotti E, Heyderman L, Nolting F, Tsukamoto A, Itoh A, Afanasiev D, Ivanov

B, Kalashnikova A, Vahaplar K, Mentink J, Kirilyuk A, Rasing T, Kimel A (2012) Ultrafast heating as a sufficient stimulus for magnetization reversal in a ferrimagnet. Nat Commun 3:666

Schieback C, Hinzke D, Kläui M, Nowak U, Nielaba P (2009) Temperature dependence of the current-induced domain wall motion from a modified Landau-Lifshitz-Bloch equation. Phys Rev B 80:214403

Schlickeiser F, Atxitia U, Wienholdt S, Hinzke D, Chubykalo-Fesenko O, Nowak U (2012) Temperature dependence of the frequencies and effective damping parameters of ferrimagnetic resonance. Phys Rev B 86:214416

Schlickeiser F, Ritzmann U, Hinzke D, Nowak U (2014) Role of entropy in domain wall motion in thermal gradients. Phys Rev Lett 113:097201

Scholz W, Schrefl T, Fidler J (2001) Micromagnetic simulation of thermally activated switching in fine particles. J Magn Magn Mat 233:296

Skubic B, Hellsvik J, Nordström L, Eriksson O (2008) A method for atomistic spin dynamics simulations: implementation and examples. J Phys Condens Matter 20:315203

Suarez O, Nieves P, Laroze D, Altbir D, Chubykalo-Fesenko O (2015) The ultra-fast relaxation rates and reversal time in disordered ferrimagnets. Phys Rev B 92:144425

Sultan M, Atxitia U, Melnikov A, Chubykalo-Fesenko O, Bovensiepen U (2012) Electron- and phonon-mediated ultrafast magnetization dynamics of Gd(0001). Phys Rev B 85:184407

Takano K, Jin E, Zhou D, Maletzky T, Smyth J, Dovek M (2011) Thermo-dynamic magnetisation model of thermally assisted magnetic recording by Landau-Lifshitz-Bloch equation. J Magn Soc Jpn 35:431

Uchida K, Takahashi S, Harii K, Ieda J, Koshibae W, Ando K, Maekawa S, Saitoh E (2008) Observation of the spin Seebeck effect. Nature 455:778

Vahaplar K, Kalashnikova AM, Kimel A, Hinzke D, Nowak U, Chantrell R, Tsukamoto A, Itoh A, Kirilyuk A, Rasing T (2009) Ultrafast path for optical magnetization reversal via a strongly nonequilibrium state. Phys Rev Lett 103:117201

Vahaplar K, Kalashnikova AM, Kimel A, Gerlach S, Hinzke D, Nowak U, Chantrell R, Tsukamoto A, Itoh A, Kirilyuk A, Rasing T (2012) All-optical magnetization reversal by circularly polarized laser pulses: Experiment and multiscale modeling. Phys Rev B 85:104402

Vogler C, Abert C, Bruckner F, Suess D (2014) Landeu-Lifshits-Bloch equation for exchange-coupled grains. Phys Rev B 90:214431

Vogler C, Abert C, Bruckner F, Suess D, Praetorius D (2016) Areal density optimizations for heat-assisted magnetic recording of high-density media. J Appl Phys 120:223903

Vogler C, Abert C, Bruckner F, Suess D (2018) Stochastic ferrimagnetic Landau-Lifshitz-Bloch equation for finite magnetic structures. arXiv:180401724

Xu L, Zhang S (2012) Magnetization dynamics at elevated temperatures. Phys E 45:72